



OPEN ACCESS

EDITED BY

Sanjay Vashee,
J. Craig Venter Institute, United States

REVIEWED BY

Yota Tsuge,
Kanazawa University, Japan
Haiwei Mou,
Wistar Institute, United States
Jia Liu,
ShanghaiTech University, China

*CORRESPONDENCE

Wei-Guo Zhang,
✉ zhangwg@jiangnan.edu.cn
Feng Zhang,
✉ xyzfjn@126.com

RECEIVED 24 October 2023

ACCEPTED 27 February 2024

PUBLISHED 12 March 2024

CITATION

Zhang F, Wang J-Y, Li C-L and Zhang W-G
(2024), HyCas9-12aGEP: an efficient genome
editing platform for
Corynebacterium glutamicum.
Front. Bioeng. Biotechnol. 12:1327172.
doi: 10.3389/fbioe.2024.1327172

COPYRIGHT

© 2024 Zhang, Wang, Li and Zhang. This is an
open-access article distributed under the terms
of the [Creative Commons Attribution License
\(CC BY\)](https://creativecommons.org/licenses/by/4.0/). The use, distribution or reproduction in
other forums is permitted, provided the original
author(s) and the copyright owner(s) are
credited and that the original publication in this
journal is cited, in accordance with accepted
academic practice. No use, distribution or
reproduction is permitted which does not
comply with these terms.

HyCas9-12aGEP: an efficient genome editing platform for *Corynebacterium glutamicum*

Feng Zhang*, Jin-Yu Wang, Chang-Lon Li and Wei-Guo Zhang*

The Key Laboratory of Industrial Biotechnology, Ministry of Education, School of Biotechnology, Jiangnan University, Wuxi, China

Corynebacterium glutamicum plays a crucial role as a significant industrial producer of metabolites. Despite the successful development of CRISPR-Cas9 and CRISPR-Cas12a-assisted genome editing technologies in *C. glutamicum*, their editing resolution and efficiency are hampered by the diverse on-target activities of guide RNAs (gRNAs). To address this problem, a hybrid CRISPR-Cas9-Cas12a genome editing platform (HyCas9-12aGEP) was developed in *C. glutamicum* in this study to co-express sgRNA (corresponding to *SpCas9* guide RNA), crRNA (corresponding to *FnCas12a* guide RNA), or hfgRNA (formed by the fusion of sgRNA and crRNA). HyCas9-12aGEP improves the efficiency of mapping active gRNAs and outperforms both CRISPR-Cas9 and CRISPR-Cas12a in genome editing resolution and efficiency. In the experiment involving the deletion of the *cg0697-0740* gene segment, an unexpected phenotype was observed, and HyCas9-12aGEP efficiently identified the responsible genotype from more than 40 genes. Here, HyCas9-12aGEP greatly improve our capability in terms of genome reprogramming in *C. glutamicum*.

KEYWORDS

active gRNA, editing resolution, hfgRNA, editing efficiency, *Corynebacterium glutamicum*

Introduction

The enzyme associated with clustered regularly interspaced short palindromic repeats (CRISPR), such as Cas9 or Cas12a, is an RNA-guided endonuclease that utilizes RNA-DNA base-pairing to identify and target foreign DNA within bacteria (Jinek et al., 2012; Zetsche et al., 2015). Guide RNA complexes with Cas9 or Cas12a are potent genome-engineering agents in both eukaryotes and prokaryotes, extensively employed in CRISPR-based methodologies (Cong et al., 2013; Jiang et al., 2013; Yan et al., 2017; Zetsche et al., 2017). For example, genetic engineering has been developed for *C. glutamicum* (Jiang et al., 2017; Liu et al., 2017; Peng et al., 2017; Wang et al., 2021; Liu et al., 2022). *C. glutamicum*, strategically engineered for industrial amino acid synthesis, serves as a versatile microorganism capable of producing a diverse range of compounds, including sunscreens, anti-aging sugars, biofuels, and polymers designed for regenerative medicine applications (Becker et al., 2018; Wolf et al., 2021). Despite being regarded as a promising tool for genome engineering in *C. glutamicum*, CRISPR-Cas9 or CRISPR-Cas12a encounters challenges primarily due to the varied on-target activities of guide RNAs (gRNAs), posing potential obstacles to its successful development.

Cas9 and Cas12a recognize distinct protospacer adjacent motif (PAM) sequences, for instance, *SpCas9* and *FnCas12a* specifically recognize 5'-NGG-3' and 5'-TTN-3',

respectively (Jinek et al., 2012; Zetsche et al., 2015). A major challenge in CRISPR/Cas9- and Cas12a-mediated genome engineering is that not all guide RNAs (gRNAs) efficiently cleave the DNA (Doench et al., 2014; Jiang et al., 2017; Kim et al., 2018; Creutzburg et al., 2020; Zhang et al., 2020; Corsi et al., 2022). Therefore, the selection and design of active gRNA are critical for CRISPR-Cas9-mediated gene editing. However, the efficacy of guide RNA (gRNA) is impacted by various factors, encompassing gRNA structure (Abdel-Mawgoud and Stephanopoulos, 2020; Creutzburg et al., 2020; Magnusson et al., 2021; Riesenberger et al., 2022), conformational transitions (Chen et al., 2017; Wang et al., 2019; Kim et al., 2020; Talas et al., 2021), R-loop formation (Gong et al., 2018), Cas9 and Cas12a variants (Chen et al., 2017; Guo et al., 2018; Wang et al., 2019; Kim et al., 2020), PAM sequences (Doench et al., 2014), supercoiling (Ivanov et al., 2020), DNA covalent modification (Tao et al., 2017; Vlot et al., 2018; Liu Y et al., 2020; Dong et al., 2021), interactions at non-targeted sites (Sternberg et al., 2014; Moreb et al., 2020), target copy number (Ivanov et al., 2020), and target accessibility (Chen et al., 2016; Horlbeck et al., 2016; Yarrington et al., 2018). Despite extensive screening of large guide RNA (gRNA) libraries and the development of algorithms to predict sequence-dependent gRNA activity (Park et al., 2021; Talas et al., 2021; Xiang et al., 2021), these algorithms exhibit limitations in accurately predicting other datasets, training datasets, or variations across different species (Moreb and Lynch, 2021). Thus, beyond the utilization of current gRNA design tools, the central challenge in gene editing resides in the experimental strategies to promptly identify active gRNAs and enhance their efficacy.

Off-target effects pose a critical challenge in CRISPR-Cas9-based gene editing and disease therapy. These effects are influenced by various factors, encompassing the quality of guide gRNA, the selection of the Cas9 protein, concentrations of both gRNA and Cas protein, cell type, and the choice of target site (Pattanayak et al., 2013; Wienert and Cromer, 2022; Guo et al., 2023). Among these factors, gRNA concentration and the level of Cas9 protein expression are the primary contributors (Hsu et al., 2013; Pattanayak et al., 2013). The effectiveness of the CRISPR-Cas9 system depends on sufficient Cas9 protein expression, as Cas9 serves as the actual nuclease responsible for gene editing. Insufficient Cas9 protein expression can impair its ability to accurately identify and cleave the target DNA, reducing editing efficiency (Pattanayak et al., 2013). Conversely, an excessive Cas9 protein concentration may lead to cleavage at off-target sites with partial sequence similarity, thereby increasing the risk of off-target effects (Hsu et al., 2013). Thus, in CRISPR-Cas9 experiments, it is essential to maintain a balanced Cas9 protein expression level to ensure efficient editing while minimizing the potential for off-target effects.

In this study, we present HyCas9-12aGEP, a system that involves the co-expression of *Streptococcus pyogenes* (Sp)-Cas9 and *Francisella novicida* (Fn)-Cas12a nucleases by integrating the *SpCas9* and *Fncas12a* genes into *C. glutamicum*. This system utilizes 'hybrid fused guide' (hfg)RNAs, generated by fusing *SpCas9* and *Fncas12a* guide RNAs and expressed from a single promoter. By reducing the expression level of *SpCas9*, HyCas9-12aGEP mitigates the off-target effects associated with *SpCas9*. In comparison to conventional CRISPR-Cas9 or Cas12a

systems, HyCas9-12aGEP, coupled with hfgRNA, markedly augments guide RNA (gRNA) activity, streamlines the identification of active gRNAs, and enhances the efficiency of gene editing. Additionally, *SpCas9* and *Fncas12a* recognize different PAM sequences, specifically 5'-NGG-3' and 5'-TTN-3', respectively. Therefore, the active gRNAs (corresponding to an active PAM) that HyCas9-12aGEP can use are the sum of *SpCas9* and *Fncas12a*, which improves the resolution of gene editing, such as precise substitution of the 149th Glycine with Lysine in the γ -glutamyl kinase encoded by *proB*. Interestingly, our experiments unveiled a notable phenotype in colonies with a 40.96 kb DNA segment (*cg0697-cg0740*) deleted from the *C. glutamicum* genome, exhibiting increased "moisture." Using HyCas9-12aGEP, genotypes that influence the phenotype were rapidly mapped from a pool of over 40 genes. In summary, HyCas9-12aGEP emerges as a potent tool for genetically modifying *C. glutamicum*, accelerating research in gene function, and optimizing the production of target products.

Materials and methods

Strains and culture conditions

Strains used in this study are listed in [Supplementary Table S1](#). *E. coli JM109*, utilized for plasmid cloning, was aerobically cultivated at 37°C in Luria-Bertani (LB) broth. The medium was supplemented accordingly with kanamycin (Kan, 50 μ g/mL) or chloramphenicol (Cm, 20 μ g/mL). *C. glutamicum* were cultured at 30°C in LBG medium (LB medium supplemented with 5 g/L glucose). The Epo medium, consisting of LBG supplemented with 3% glycine, 0.1% Tween 80, and 0.4% isoniazid, was utilized for cultivating electroporation-competent cells. LBHIS medium, containing 2.5 g/L yeast extract, 5 g/L tryptone, 5 g/L NaCl, 18.5 g/L Brain Heart Infusion powder, and 91 g/L sorbitol, were employed to obtain transformants of *C. glutamicum*, following previously described procedures (Xu J et al., 2014). The CM medium (10 g/L yeast extract, 10 g/L beef extract, 10 g/L tryptone, 5 g/L glucose, and 5 g/L NaCl) is utilized for colony phenotype observation on agar plates. Kan (25 μ g/mL) was added to LBHIS medium as required.

Plasmid construction

Plasmids utilized in this study are listed in [Supplementary Table S2](#) and [Supplementary Data S1](#). Plasmids were constructed via recombination or T4 DNA ligase. Recombination was conducted using the ClonExpress II and ClonExpress MultiS One Step Cloning Kit (Vazyme, Nanjing, China). Restriction endonucleases and T4 DNA ligase were purchased from TaKaRa (Dalian, China). DNA polymerase and reagents were purchased from Vazyme (Nanjing, China). Gene synthesis and DNA sequencing were provided by GENEWIZ Inc. (Suzhou, China). Primers synthesized by Exsyn-bio (Wuxi, China) and details for constructing plasmids are described in [Supplementary Data S1](#).

Design of gRNAs

The general sgRNAs were designed via online software (<http://www.rgenome.net/cas-designer/>) (Park J and Kim, 2015). The relevant sgRNA sequences are listed in Supplementary Data S2.

Genome editing in *C. glutamicum*

The traditional pK18*mobsacB*-based gene deletion and insertion were performed as previously described (Xu J et al., 2014). HyCas9-12aGEP has been successfully applied in genome editing, and the detail progress are listed in the Supplementary methods (Supplementary Material). In this study, the size of homologous arm (HA) carried by plasmid pZF2 was -1 kb.

The preparation of competent *C. glutamicum* was carried out following the previously described method with appropriate modifications (Liu et al., 2022). The strains were cultured in 50-mL shake flasks with 10 mL of LBG media for 10–13 h, and then 3 mL was transferred to 100 mL of Epo media in 500-mL shake flasks for 30°C-cultivation. When the ΔOD_{600} of the culture reached to 0.4–0.5, the culture were ice-bathed for 15–20 min and were then harvested through 5-min centrifugation at 4°C and 4,000 rpm. The cells were subsequently resuspended in 300–500 μ L of 10.0% (v/v) glycerol after washing 3 times using 4°C pre-chilled 10% glycerol. The plasmid was mixed with competent cells and subsequently introduced into an electroporation cuvette. Electroporation was carried out utilizing an GenePulser Xcell™ (Bio-Rad Laboratories, Shanghai, China) with parameter settings of 1800 V, 5 ms, and 1 mm. Subsequently, 800 μ L of LBHIS media was immediately added, followed by rapidly 6-min incubation of the suspension at 46°C. The cells were 2-h cultured at 30°C, and then spread on LBHIS plates containing antibiotics for 30°C-incubation until the appearance of colonies.

Re-sequencing analysis

Re-sequencing was conducted to identify off-target occurrences in the edited strains. Referring to the previously described method (Peng et al., 2017). Total DNA from *C. glutamicum* was extracted following the manufacturer's protocol provided by Vazyme, Nanjing, China. The assessment of DNA quality involved utilizing the Qubit Fluorometer (Thermo Fisher Scientific, San Jose, CA, United States) for measuring overall mass and the Fragment Analyzer for evaluating DNA integrity. The genomic sequencing was executed utilizing the Illumina HiSeq/Nova 2 \times 150bp system (Illumina, San Diego, CA, United States) at the GENEWIZ Inc. (Suzhou, China).

Plasmid curing

For plasmid curing, transformants were grown in antibiotic-free LBG medium at 37°C overnight (-8 h) and subsequently plated on antibiotic-free CM plates. The next day, the culture is diluted and coated into kanamycin-resistant CM plates and cultured at 30°C. Plasmid curing was judged by the colony's sensitivity to antibiotics.

The grown single colonies were transferred to one CM kanamycin-resistant plate and the corresponding CM plate, respectively. Single colonies that cannot be grown in response to resistant plates are plasmid eliminated successfully for the next round of gene editing or other tests.

RT-PCR for mRNA quantification

RT-qPCR assay was performed as described previously (Wang et al., 2020). To determine the transcriptional intensity of *Spcas9* or *Fncas12a* in the seven *Spcas9* or *Fncas12a*-expressing strains, i.e. 9-12, E9-12, L9-12, 9-E12, 9-L12, Cas9-2, and Cas12-2, quantitative reverse transcription PCR (qRT-PCR) was performed using total RNA samples. Total RNA was isolated from the cells with the RNAprep Pure Cell/Bacteria Kit (Tiangen, China). 0.5 μ g of the total bacterial RNA was subjected to reverse transcription using the HiScript II Q RT SuperMix Kit (Vazyme). RT-qPCR analysis using the ChamQ Universal SYBR qPCR master mix kit (Vazyme) in a total reaction volume of 20 μ L in a CFX96™ Real-Time System (Bio-Rad, Hercules, CA, United States). The 16S rRNA encoding gene was used as an internal control as described previously (Pan et al., 2022). PCR primers used in RT-PCR are listed in Supplementary Data S1.

Analytical methods

Cell growth was calculated by measuring the optical density at 600 nm (OD_{600}) using a spectrophotometer (Shanghai, China). Cell morphology was examined using field emission scanning electron microscopy (FESEM). *C. glutamicum* cells were harvested by centrifugation, washed thrice with physiological saline (pH 7.0), and subsequently deposited onto a small silicon platelet. After air-drying at room temperature, the cells underwent *in-situ* fixation with a 2.5% glutaraldehyde solution in a 0.15 M sodium phosphate buffer (pH 7.4) for 10 min. The samples were gold-coated and examined under field emission scanning electron microscopy (FESEM) using a Hitachi SU8220 instrument with an accelerating voltage of 3 kV.

Statistical analysis

All experiments were conducted with three independent replicates. Statistical analysis of the data was carried out using t-tests in SPSS v.25. A significance threshold of $p < 0.05$ was applied, and the level of significance is denoted as $***p < 0.01$.

Results

Exploration of gene editing system to broaden the target range

The success of CRISPR gene editing applications relies significantly on the presence of active gRNAs. SpRY-Cas9 (Walton RT et al., 2020) is an unconstrained near-PAMless

genome, and SpCas9-HF1 (Chen et al., 2017) is high-fidelity SpCas9 variant. Thus, the mutant SpRY-HF1 obtained by combining SpRY-Cas9 and SpCas9-HF1 was inferred to increase the density of active gRNAs and to improve editing resolution. Thus, the open reading frame (ORF) of SpCas9 in pFSC (Peng et al., 2017) was replaced with the codon-optimized ORF of SpRY-HF1 (NCBI accession numbers: OP345224) to obtain the plasmid pXMJ19-SpRY-HF1. Subsequently, a plasmid, pFST-porB-HD (Peng et al., 2017), carrying active gRNA targeting *porB* and two homologous arms of -1 kb each, was electroporated into *C. glutamicum* ATCC13032 harboring the plasmid pXMJ19-SpRY-HF1. Although SpRY-HF1 exhibited high expression (Supplementary Figure S1A), it indicated an exceedingly low counter-selection efficiency (Supplementary Figure S1B), which may be attributed to the excessive number of mutation sites that tend to reduce nuclease activity (Okafor et al., 2019) or increase off-target titration in the genome (Moreb and Lynch, 2021). This results in the extension of the search times for targeted loci, and in turn, leads to a reduction in counter-selection efficiency. Hence, this indicates that the gene editing application of the SpCas9 variant SpRY-HF1 in *C. glutamicum* still requires further optimization.

Development and optimization of a hybrid CRISPR-Cas9-Cas12a gene editing platform

SpCas9 and Fncas12a recognize different PAM sequences of 5'-NGG-3' and 5'-TTN-3' respectively (Jinek et al., 2012; Zetsche et al., 2015). Therefore, incorporating both SpCas9 and Fncas12a into a unified system facilitates the broadening of the targeting range. Considering this, 2 *C. glutamicum*-*E. coli* shuttle plasmids were constructed based on the plasmids pFSC (Peng et al., 2017) and pJYS3 (Jiang et al., 2017): pFSC-Cas12a and pJYS3-Cas9, which carried the P_{lacM} -Fncas12a-rrnBT1T2-Spcas9- P_{tac} cassette and were transformed into *C. glutamicum* ATCC 13032 (i.e., 13032). However, this yielded no transformants (Supplementary Figure S1B). It has been reported that constitutive expression of plasmid-borne dCas9 from *S. pyogenes* in *C. glutamicum* has proven to be unattainable (Cleto et al., 2016). Thus, it was speculated that this may be due to the oversized plasmid vector and the simultaneous expression of the two Cas nucleases, resulting in a superposition of toxicity. To address these challenges, the P_{tac} -SpCas9-rrnBT1T2 and P_{lacM} -Fncas12a-rrnBT1T2 cassettes were integrated into the 13032 genome at the *putA* and *ldh* gene loci, resulting in strains Ptac-9 and L12, respectively (Supplementary Figure S2A). The strains with two Cas-coding gene copies were then constructed to obtain the following: 9-12 with one copy each of P_{tac} -Spcas9-rrnBT1T2 and P_{lacM} -cas12a-rrnBT1T2, Cas9-2 with two copies of P_{tac} -Spcas9-rrnBT1T2, and Cas12a-2 with two copies of Fncas12a (Supplementary Figure S2A; Supplementary Table S3). In this growth experiment, it was observed that by integrating a single copy of the P_{tac} -Spcas9-rrnBT1T2 and P_{lacM} -Fncas12a-rrnBT1T2 into the genome, the growth of strain 13032 was hardly affected, whereas, growth was significantly inhibited when two copies of the P_{tac} -Spcas9-rrnBT1T2 and P_{lacM} -Fncas12a-rrnBT1T2 were integrated (Supplementary Figure S2B). Hence, nuclease-induced toxicity can be entirely removed in the

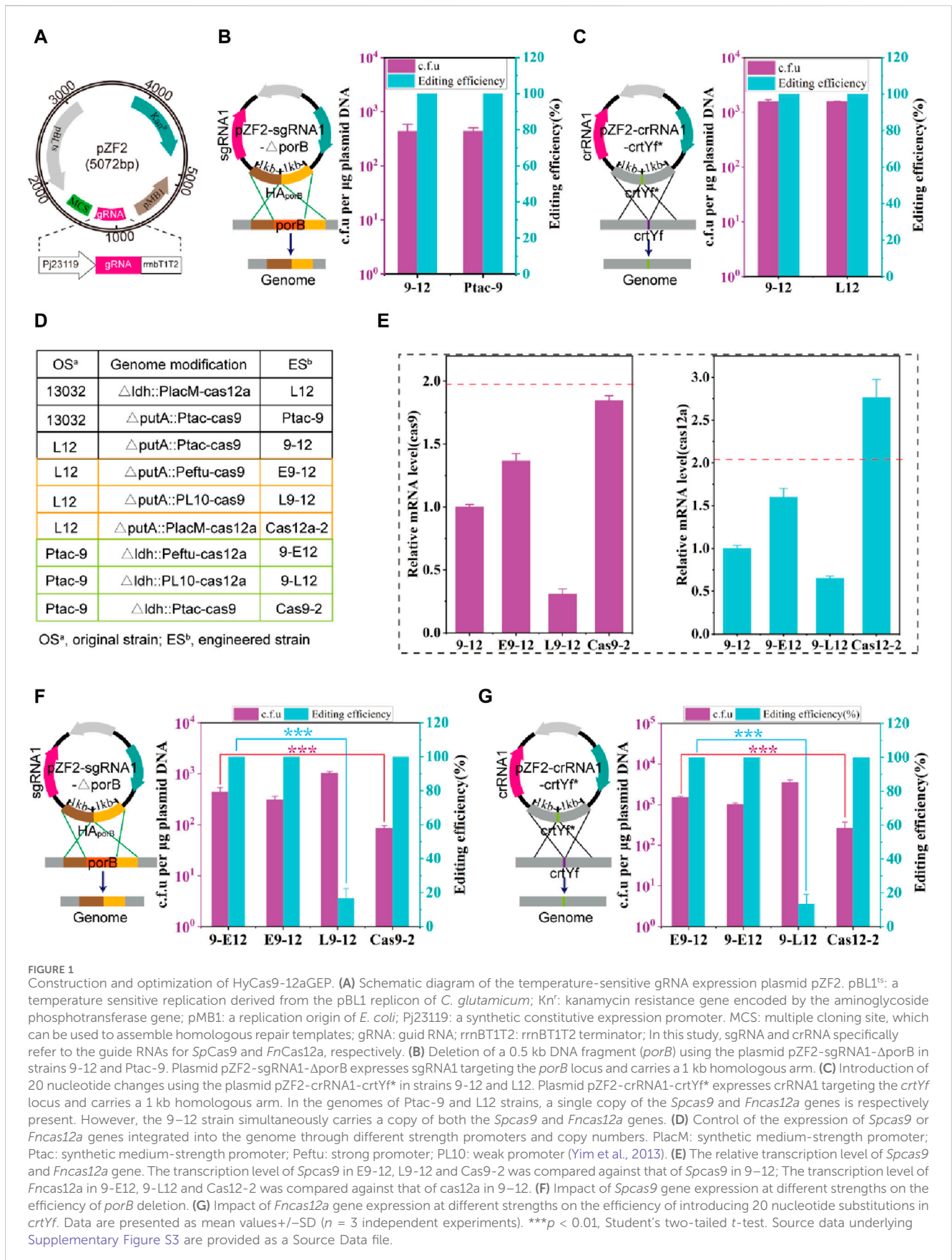
13032 when genomic integration uses a single copy of the P_{tac} -Spcas9-rrnBT1T2 and P_{lacM} -Fncas12a-rrnBT1T2.

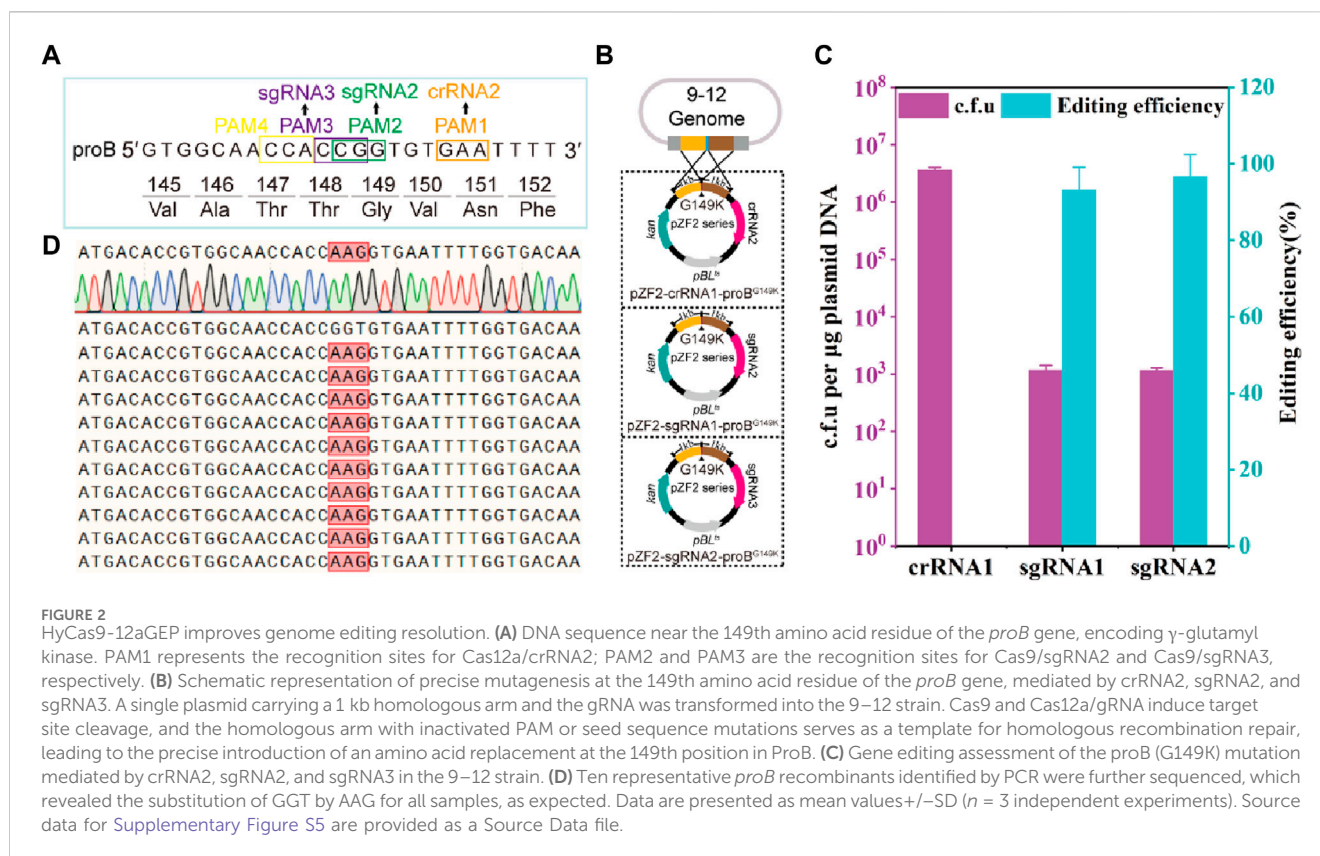
Next, the genome-editing performance of the hybrid CRISPR-Cas9-Cas12a system was tested. A temperature-sensitive plasmid, pZF2, was initially designed for expressing the gRNA and harboring homologous arms (HA) (Figure 1A). It has been reported that crRNA-crtYf (Jiang et al., 2017) (crRNA1) and sgRNA-porB (Peng et al., 2017) (sgRNA1) facilitate highly effective gene editing. Thus, crRNA1 and sgRNA1 are assembled into plasmids pZF2 harboring the corresponding homologous arms, obtaining plasmids pZF2-sgRNA1- Δ porB and pZF2-crRNA1-crtYf*, which are used to knock out the gene *porB* (0.5 kb) and introduce point mutations at the *crtYf* site, respectively. The two plasmids were then transformed to 9-12 strain, and the colony PCR results showed that the knockout of *porB* and the point mutation efficiency of *crtYf* reached 100% (Figures 1B,C; Supplementary Figure S3), which was comparable to the optimal editing efficiency previously reported (Jiang et al., 2017; Peng et al., 2017). The strains that were successfully edited were subsequently cultured overnight at 37°C, resulting in plasmid curing efficiencies of approximately 100% (Supplementary Figure S4).

The expression level of Cas proteins is a critical factor influencing editing efficiency (Hsu et al., 2013; Pattanayak et al., 2013). Thus, various strategies, including the replacement of Cas gene promoters and increasing copy numbers (Figure 1D), were employed to optimize the expression levels of Cas genes. A series of *C. glutamicum* carrying the HyCas9-12aGEP were developed, utilizing either a strong P_{eftu} promoter or a weak P_{L10} (Yim et al., 2013) promoter to regulate the expression of Spcas9 and Fncas12a (Figure 1D). As expected, the transcription levels of Spcas9 and Fncas12a were consistent with the strength of their respective promoters (Figure 1E). Notably, compared to 9-12, the transcription levels of Fncas12a and Spcas9 in Cas12a-2 and Cas9-2 were increased by 176% and 84%, respectively (Figure 1E), suggesting that the location of genes in the genome affects the expression of genes (Akhtar et al., 2013; Bryant et al., 2014; Goormans et al., 2020). Transformation with 1 μ g of pZF2-sgRNA1- Δ porB into L9-12, produced more than 10^3 c.f.u., among which \sim 16.6% were correctly edited (Figure 1F). However, compared to 9-E12, Cas9-2 exhibited similar editing efficiency but a significantly reduced number of transformants (Figure 1F). Similar results were observed when the plasmid pZF2-crRNA1-crtYf* was transformed into strains containing cas12a genes controlled by promoters of varying strengths (Figure 1G). These results indicate that insufficient expression levels of SpCas9 and Fncas12a result in a high escape rate that is inadequate for eliminating wild-type cells, while excessively high expression levels of SpCas9 and Fncas12a lead to reduced transformation efficiency. Therefore, the 9-12 strain, which balances transformation efficiency and editing efficiency, was selected for subsequent experiments.

HyCas9-12aGEP improves genome editing resolution

Due to the heterogeneity of gRNA activity, there are instances where no active gRNA is available for specific gene loci, leading to a





decrease in the resolution of gene editing. For example, CRISPR-*FnCas12a* (Jiang et al., 2017) and *SpCas9* (Zhang et al., 2020) have been reported to lack suitable gRNAs for specific gene loci in *proB* and *zwf*, respectively, resulting in failures to precisely introduce mutations at the target gene sites in *C. glutamicum*. Thus, this generally lowers the resolution of CRISPR-Cas-based gene editing compared to the theoretical value. However, by leveraging both *SpCas9* and *FnCas12a* nucleases, each recognizing different PAM sequences, HyCas9-12aGEP increases gRNA availability, thereby enhancing gene editing resolution.

The γ -glutamyl kinase encoded by *proB* is the rate-limiting enzyme in proline synthesis and is subject to feedback inhibition by proline (Perez-Arellano et al., 2006; Wendisch, 2014). Using CRISPR-Cas12a-assisted genome editing, the mutant strain 13032ProB^{G149K} was generated to alleviate the feedback inhibition of proline, involving the introduction of adjacent synonymous mutations (Jiang et al., 2017). However, it has been reported that synonymous mutations do not alter the encoded protein but can influence gene expression (Kudla et al., 2009). Thus, to prevent the introduction of synonymous mutations, theoretically, only 1 PAM is available for *FnCas12a* to introduce site-directed mutations at the 149th amino acid residue of ProB, while *SpCas9* has 3 available PAMs (Figure 2A). Here, crRNA2, sgRNA2 and sgRNA3 are inactivated by mutation of the 149th amino acid residue glycine (GGT) of CgProB in the homologous arm to lysine (AAG). Thus, the plasmids pZF2-crRNA2-ProB^{G149K}, pZF2-sgRNA2-ProB^{G149K}, and pZF2-sgRNA3-ProB^{G149K} are created by assembling crRNA2, sgRNA2, sgRNA3 and homology arms into the plasmid pZF2 (Figure 2B). The *FnCas12a*-based edited plasmid pZF2-crRNA2-

ProB^{G149K} was electroporated into the 9–12 strain, and no transformants containing the ProB^{G149K} mutation were detected (Figure 2C), potentially attributed to insufficient crRNA2 activity (Figure 2C). However, *SpCas9*-based editing plasmids pZF2-sgRNA2-ProB^{G149K} and pZF2-sgRNA3-ProB^{G149K} were transformed into the 9–12 strain, produced $\sim 1.1 \times 10^3$ c.f.u., among which $\sim 93.3\%$ and 96.6% were correctly edited, respectively (Figures 2C; Supplementary Figure S5). The mutated transformants were subsequently further verified by sequencing (Figure 2D). Thus, these results suggest that the HyCas9-12aGEP enables more precise mutations than the CRISPR-Cas12a system, thereby improving gene editing resolution. Furthermore, these findings emphasize the importance of active gRNAs in successful gene editing.

HyCas9-12aGEP improves the mapping efficiency of active gRNAs

The efficiency of CRISPR-based gene editing is highly dependent on gRNA activity (Figure 2C). Therefore, the selection and design of efficient gRNAs is essential to improve gene editing efficiency. Although tools have been developed to predict gRNA activity in certain hosts, these programs still have limitations in accurately predicting gRNA activity in diverse hosts because different cells and host types are also factors affecting gRNA activity (Moreb and Lynch, 2021). Literature mining is an effective strategy, but the targets of gRNA used in the literature are limited, which is difficult to meet the requirements of different experimental content. Therefore,

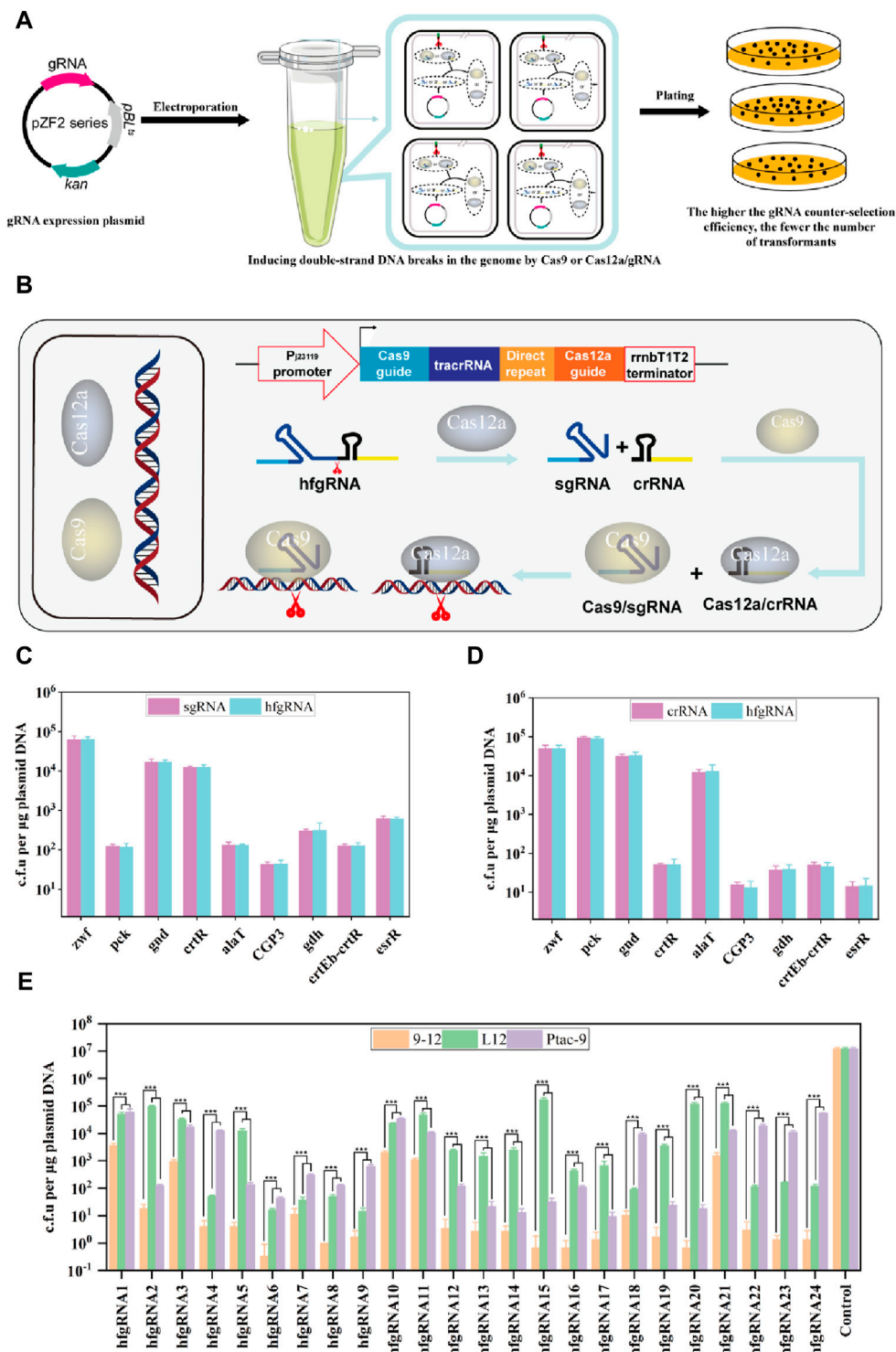


FIGURE 3 Determination of gRNA activity through experimental methods. **(A)** Schematic representation of gRNA activity assessment based on experiments. I: Plasmids carrying gRNAs were transformed into Ptac-9 (CRISPR-Cas9), L12 (CRISPR-Cas12a), and 9-12 (HyCas9-12aGEP); II: Expressed gRNAs guide Cas9 or Cas12a for genome cleavage; III: The more thorough the cleavage of genomic DNA by Cas9/gRNA or Cas12a/gRNA, the fewer the number of transformants. **(B)** Schematic representation of dual-target DNA cleavage mediated by hfgRNA in 9-12. Transformed hfgRNA is processed by Cas12a to yield crRNA and sgRNA, guiding Cas12a and Cas9 to simultaneously target two genomic loci. **(C, D)** Impact of hfgRNA design on the activity of sgRNAs and crRNAs targeting the *zwf*, *pck*, *gnd*, *crtr*, *alaT*, *CCP3*, *gdh*, *crfEb-crtr* and *esrR* loci. Plasmids expressing sgRNA, crRNA, and their respective fusion hfgRNA were separately transformed into Ptac-9 and L12 to determine the number of transformants. **(E)** Determination of the transformation efficiency of 24 hfgRNAs in Ptac-9, L12, and 9-12. The 24 corresponding target sites for hfgRNAs are provided in Supplementary Data S2. hfgRNA1-9 are used in panels **(C)** and **(D)**. Data are presented as mean values ± SD ($n = 3$ independent experiments). *** $p < 0.01$, Student's two-tailed t-test.

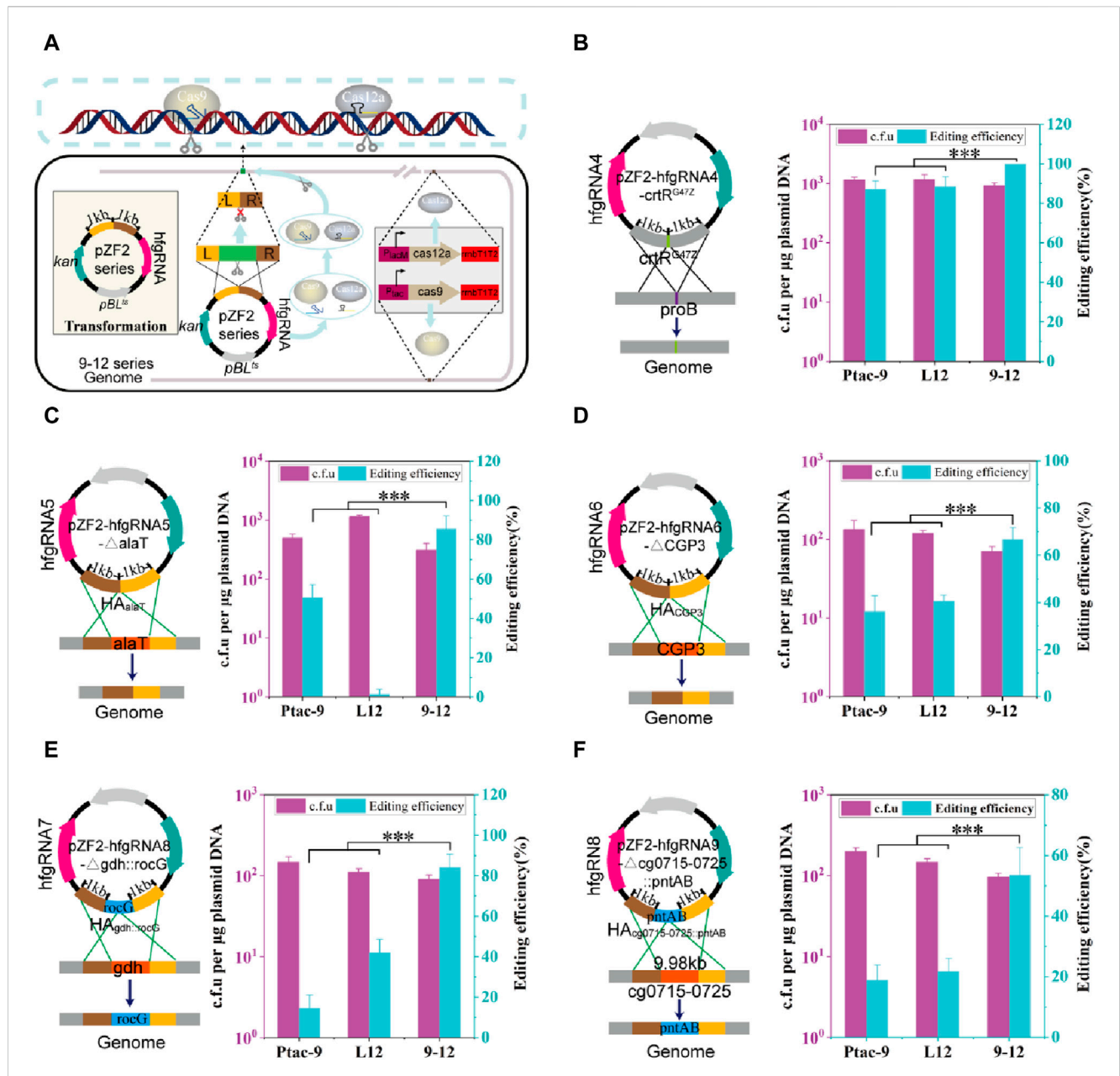


FIGURE 4 Genome editing mediated by hfgRNA in CRISPR-Cas9, CRISPR-Cas12a, and HyCas9-12aGEP. (A) Schematic representation of gene editing mediated by hfgRNA in the HyCas9-12aGEP system. The transcribed hfgRNA is processed by *Fn*Cas12a to generate crRNA and sgRNA, which respectively guide *Fn*Cas12a and *Sp*Cas9 to simultaneously target and cleave two distinct loci in the genome. Homologous recombination is employed for the introduction of the desired mutations. (B–F) Genome editing using hfgRNA in the 9–12 strain harboring HyCas9-12aGEP. hfgRNA4–8 are designed to target *crtR*, *alaT*, CGP3, *gdh*, and *crtR/crtE*, for the introduction of mutations including *crtR*G47Z, Δ*alaT* (0.5 kb), ΔCGP3 (219 kb), Δ*gdh*rocG, and Δ*cg0715–0725*pntAB. *CrtR*^{G47Z} involves the substitution of the 47th glycine residue in *CrtR* with a stop codon to deactivate the *crtR* gene. Δ*alaT* (0.5 kb): deletion of a 0.5 kb segment of the *alaT* gene. ΔCGP3 (219 kb): the complete removal of the CGP3 bacteriophage, spanning 219 kb Δ*gdh*rocG: deletion of the endogenous glutamate dehydrogenase gene *gdh* (1.34 kb) and concomitant insertion of the expression cassette *Ptac-rocG-rrnBT1T2* (1.58 kb), encoding the glutamate dehydrogenase *rocG* derived from *Bacillus subtilis*. Δ*cg0715–0725*pntAB: deletion of the gene cluster *cg0715–0725* while inserting the expression cassette PH36-pntAB-rrnBT1T2 (3.5 kb) from *E. coli*. Data are presented as mean values ± SD (*n* = 3 independent experiments). ****p* < 0.01, Student’s two-tailed *t*-test. Source data underlying Supplementary Figure S6 are provided as a Source Data file.

efficiently mapping active gRNA remains a bottleneck in CRISPR-Cas gene editing experiments.

Next, we attempted to establish a method for evaluating gRNA activity through experimental assays. It is widely recognized that non-homologous end joining (NHEJ) and homologous recombination (HR) are the primary repair pathways for DNA

double-strand breaks. However, it should be noted that the NHEJ pathway is impaired in *C. glutamicum* (Resende et al., 2011) (<https://www.kegg.jp/kegg/pathway.html>). When gRNA guides *Sp*Cas9 or *Fn*Cas12a to cleavage DNA, in the absence of a homologous repair template, the organism undergoes cell death since the double-stranded DNA break cannot be repaired. Therefore, gRNA

activity can be assessed through the transformation efficiency of gRNA expression plasmids lacking homologous repair templates. In other words, higher gRNA activity leads to more efficient SpCas9/gRNA DNA cleavage, resulting in fewer corresponding transformants, and *vice versa* (Figure 3A). Since *FnCas12a* can process its own crRNA, transcribed hfgRNA can be processed into independent crRNA and sgRNA, which can orthogonally guide *SpCas9* and *FnCas12a* to target two genomic loci (Figure 3B). This allows a single hfgRNA to assess the targeting activity of two designed gRNAs, doubling the efficiency of identifying active gRNAs. As a proof of concept, nine crRNAs and sgRNAs targeting the *zwf*, *pck*, *gnd*, *crtR*, *alaT*, phage CGP3, *gdh*, *crtEb-crtR* and *esrR* loci, were transcribed individually or co-transcribed with their respective nine hfgRNAs. Unexpectedly, we did not observe a significant difference in the counter-selection efficiency of hfgRNA in Ptac-9 and L12 when compared to independently transcribed sgRNA and crRNA (Figures 3C,D). These results suggested that hfgRNA design does not affect the activity of sgRNA or crRNA, thereby confirming that HyCas9-based approaches can indeed improve the efficiency of identifying active gRNAs. Notably, the counter-selection efficiency achieved with hfgRNA in strain 9–12 exhibited a significant enhancement compared to Ptac-9 and L12 (Figure 3E). Similarly, based on the gRNA online design tool (<http://www.rgenome.net/cas-designer/>), we designed 15 crRNAs and 15 sgRNAs and assembled them into corresponding hfgRNAs (Supplementary Data S1, S2), which can also significantly improve the counter-selection efficiency in 9–12 (Figure 3E). These results suggested that hfgRNA based on HyCas9-12aGEP can also improve the counter-selection efficiency.

HyCas9-12aGEP combined with hfgRNA improves the genome editing efficiency

Based on HyCas9-12aGEP, hfgRNA effectively improves the counter-selection efficiency (Figure 3E). To test hfgRNA gene editing performance, plasmids expressing hfgRNA and harboring two ~1 kb HAs were transformed into 9–12, Ptac-9, and L12 strains (Figure 4A). First, hfgRNA4 was used to introduce a stop codon into the *crtR* gene to inactivate CrtR (CrtR^{G47Z}). Although the site-directed mutation efficiency of hfgRNA4 in Ptac-9 and L12 is as high as 86.9% and 88.4%, respectively, the editing efficiency reached 100% in 9–12 (Figure 4B). Similarly, when hfgRNA5 was used to delete the 0.5 kb *alaT* gene in 9–12, an editing efficiency of 85.5% was obtained, which was significantly higher than the 50.7% and 1.44% obtained in Ptac-9 and L12 (Figure 4C). Notably, when hfgRNA6 was employed in Ptac-9 and L12 to delete a 219 kb DNA fragment (intact phage CGP3), editing efficiencies of 36.2% and 40.6% were achieved, respectively, slightly exceeding the 34.8% efficiency previously reported (Liu et al., 2022) (Figure 4D). However, when the CGP3 (219 kb) was deleted in strains 9–12, an editing efficiency of 66.6% was achieved, surpassing the levels attainable in Ptac-9 and L12 (Figure 4D).

Next, we tested the editing efficiency of hfgRNA in insertion. To optimize chemical and biofuel production, strategies in cofactor engineering have been devised, including adjustments in cofactor supply and modifications to reactants' cofactor preference, ensuring redox balance (Wang et al., 2017). Thus, hfgRNA7 was used to delete

the NADPH-dependent glutamate dehydrogenase gene *gdh* (1.34 kb) deletion in *C. glutamicum*, while insert the NADH-dependent glutamate dehydrogenase gene *rocG* (1.58 kb) from *Bacillus subtilis* 168. The editing efficiency of hfgRNA5 in Ptac-9 and L12 was 14.5% and 42.0%, respectively, but it was as high as 84.0% in 9–12 (Figure 4E). Finally, we also test whether hfgRNA8 can achieve deletion of large fragments (9.98 kb) while inserting the *E. coli*-derived *pntAB* (3.5 kb) operon. The membrane-bound transhydrogenase encoded by *pntAB* is advantageous for enhancing the supply of NADPH, thereby promoting the synthesis of high-value metabolic products (Kleine et al., 2017). Notably, hfgRNA6 achieved a deletion-insertion efficiency of 53.6% in 9–12 strain, significantly higher than Ptac-9 and L12, which yielded efficiencies of 18.8% and 21.7%, respectively (Figure 4F). In conclusion, the above results suggested that hfgRNA significantly improves the efficiency of genome editing based on HyCas9-12aGEP.

Application of the HyCas9-12aGEP for efficient phenotype-genotype mapping

Large fragment genome editing can be used to study the function of genes and noncoding regions. By deleting large DNA fragments, researchers can gain profound insights into how these regions impact an organism's growth, development, and physiological processes. The complete *crtREBIYe/ffEb* gene cluster (*cg0717-0725*) is an important factor in the yellow color of *C. glutamicum*, and deletion of the *cg0717-0725* may cause the color of the organism to change (Figure 5A). Here, hfgRNA8 was used to performed large fragment gene deletion testing of *cg0715-0725* (9.98 kb), *cg0715-0736* (20.02 kb) and *cg0697-cg0740* (40.96 kb) (Figure 5B). For deletion of *cg0715-0725*, transformants of two colony morphologies, white and yellow, were obtained (Supplementary Figure S7A). The white single clones were picked for PCR verification, and the results showed that they were all successfully edited strains (Supplementary Figure S7B). Hence, the success of editing can be determined by the color of individual colonies (Supplementary Figures S7B, S8A). As expected, hfgRNA8 significantly improved editing efficiency in 9–12 compared to Ptac-9 and L12 (Figure 5C; Supplementary Table S3). Remarkably, the deletion of 40.9 kb failed to yield detectable successfully edited strains in L12 and Ptac-9, whereas 9–12 maintained a remarkable editing efficiency of 38.1%. Unexpectedly, the deletion of the 40.9 kb fragment altered the colony morphology, rendering it more "moisture" (Figure 5D). However, no significant changes in the morphology of the bacteria were found by electron microscopy (Figure 5E). Therefore, we inferred that this phenotype may be caused by significant metabolic changes.

Next, we performed gradual gene fragment deletions to identify phenotype-influencing genes (Figure 5F). Since the expected phenotype didn't emerge with the 20 kb gene fragment knockout, the gene affecting the phenotype likely resides in the 20–40 kb region. Deleting the 29.86 kb DNA fragment (47.2% editing efficiency) revealed the phenotype (Supplementary Figure S8B), pinpointing the gene affecting it in the 20–30 kb range. Notably, the three-component system *EsrISR* (encoded by *cg0706-0708*)

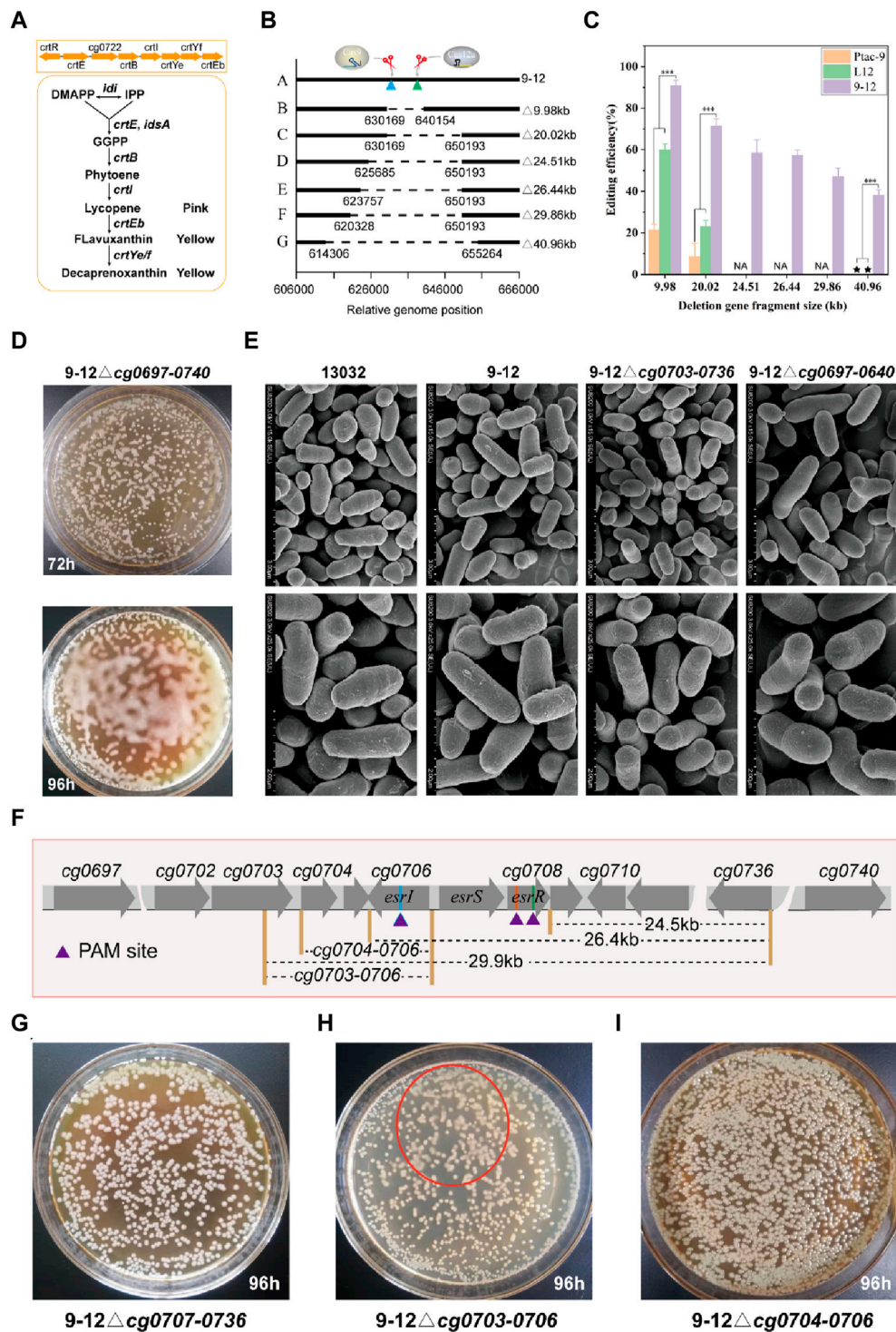
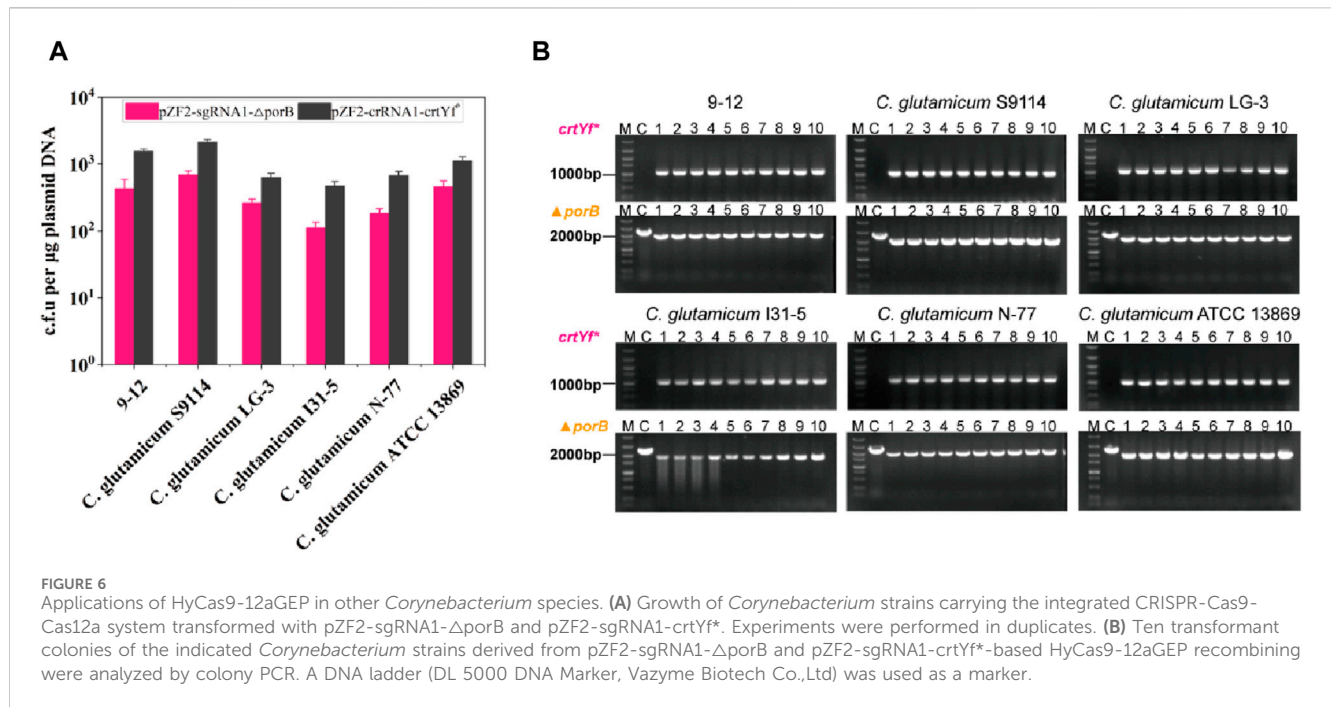


FIGURE 5 Application of HyCas9-12aGEP for phenotype-genotype mapping via large DNA segment deletion. **(A)** The reaction catalyzed by the *crtEBIYe/fEb* gene cluster for terpenoid biosynthesis. DMAPP: dimethylallyl pyrophosphate; IPP: isopentenyl pyrophosphate; GGPP: geranylgeranyl diphosphate; **(B)** Relative genomic positions of *cg0725-0725* (9.98 kb), *cg0715-0736* (20.02 kb), *cg0710-0736* (24.51 kb), *cg0707-0736* (26.44 kb), *cg0703-0736* (29.86 kb), and *cg0697-0740* (40.96 kb) in *C. glutamicum* ATCC13032. **(C)** Deletion efficiency of *cg0725-0725* (9.98 kb), *cg0715-36* (20.02 kb), *cg0710-0736* (24.51 kb), *cg0707-0736* (26.44 kb), *cg0703-0736* (29.86 kb), and *cg0697-0740* (40.96 kb) guided by hfgRNA8. **(D)** Phenotypic changes induced by the deletion of *cg0697-0740* (40.96 kb) in *C. glutamicum*. Deletion of *cg0697-0740* (40.96 kb) leads to increased ‘moisture’ of *C. glutamicum* on CM agar plates. **(E)** Scanning electron microscopy results of five different genotypes of **(C)** *C. glutamicum*, including 13032, 9-12, 9-12 Δ cg0703-0736, and 9-12 Δ cg0697-0740. **(F)** Phenotype-genotype mapping strategy. Rapid phenotype-genotype mapping is achieved through a strategy of halving the number of genes each time to pinpoint the genotypes responsible for the observed phenotypic changes. **(G–I)** Colony phenotypes of 9-12 Δ cg0707-0736, 9-12 Δ cg0704-0706, and 9-12 Δ cg0703-0706 on CM agar plates after 96 h, respectively. The red ellipse indicates the corresponding ‘moisture’ colony phenotype observed in 9-12 Δ cg0703-0706. Data are presented as mean values \pm SD ($n = 3$ independent experiments). *** $p < 0.01$, Student’s two-tailed t -test. Source data underlying Supplementary Figure S7 and Supplementary Table S3 are provided as a Source Data file.



regulates a cell envelope stress response in *C. glutamicum* (Kleine et al., 2017). However, sequential deletions of *cg0710-0736* (24.51 kb) and *cg0707-0736* (26.44 kb) fragments did not induce the same phenotype (Figure 5G), which suggested that the EsrISR three-component system has an extremely limited contribution to this phenotype, and deletion experiments of *cg0706-0708* using hfgRNA9 also support this finding (Supplementary Figures S8C, D). Thus, only *cg0703-0706* remained unevaluated. Finally, crRNA11 was employed to target *esrI* (*cg0706*) and facilitate the deletion of *cg0703-0706*, resulting in the strain 9-12 Δ *cg0703-0706* (Supplementary Figure S8D), which exhibited a milder version of the phenotype compared to the 29.86 kb and 40.96 kb deletions (Figure 5H). Moreover, 9-12 Δ *cg0704-0706* strain did not yield the expected phenotype (Figure 5I; Supplementary Figure S8D). Thus, it can be inferred that the deletion of *cg0703* is responsible for this phenotype, but the deletion of *cg0704-0736* also greatly contributed to it. The precise regulatory mechanism can be further elucidated through subsequent transcriptomic and metabolomic analyses. In conclusion, based on HyCas9-12aGEP, hfgRNA enables efficient phenotype-genotype mapping.

Applicability of HyCas9-12aGEP in other *Corynebacterium* species

To determine whether HyCas9-12aGEP can be constructed in other species of *Corynebacterium* except for strain 13032, the HyCas9-12aGEP was introduced into strains *C. glutamicum* S9114, *C. glutamicum* ATCC 13869, *C. glutamicum* LG-3, *C. glutamicum* N-77, and *C. glutamicum* I31-5 by sequentially integrating the *Cas12a* and *SpCas9* genes at the *ldh* and *putA* locus of these strains genome. Plasmids pZF2-sgRNA1- Δ porB and pZF2-crRNA1-crtYf* were transformed to a series of strains harboring HyCas9-12aGEP to evaluate the editing efficiency.

Although differences in transformation efficiency were observed among different strains harboring HyCas9-12aGEP (Figure 6A), all six tested strains exhibited comparable editing efficiency for the target loci (Figure 6B). Hence, these results suggested that the HyCas9-12aGEP system can be applied to other species of *Corynebacterium*.

Off target analysis of HyCas9-12aGEP

To analysis the off-target effect in *C. glutamicum* after gene editing by HyCas9-12aGEP, genome resequencing was performed to identify all the single nucleotide polymorphism (SNP) and insertions and deletions (Indel). The strains analyzed included 9-12 Δ *porB* (*porB*-deleted strain), 9-12 Δ *cg0697-0740* (*cg0697-0740*-deleted strain) and the 9-12 Δ *gdh::rocG* (*gdh*-deleted and *rocG*-inserted strain), with wild-type 13032 serving as the negative control. Furthermore, to investigate whether the *SpCas9* and *FnCas12a* protein induce off-target effects in the absence of gRNA, the SNP and Indel profiles of the 9-12 strain harboring *SpCas9* and *FnCas12a* proteins were also examined. The results indicated that no off-target mutations were identified in the 9-12 strain containing *SpCas9* and *FnCas12a* proteins. That is, in comparison to the wild-type strain, only two Indels (corresponding to *ldh* and *putA* deletions) and two intergenic Indels (corresponding to *SpCas9* and *FnCas12a* integrations) were detected, with no SNPs observed in this strain. Meanwhile, No SNP and Indel were identified in the 9-12 Δ *cg0697-0740* and 9-12 Δ *gdh::rocG* strains (Supplementary Table S4). Notely, compared to previous reports where 1 Indel with 1 base deleted was identified during the resequencing of *porB*-deleted strains (Peng et al., 2017), we did not observe any SNP and Indel in the 9-12 Δ *porB* strains

(Supplementary Table S4). The results suggested that the genomic integration of the *SpCas9* gene effectively reduces the off-target effects of *SpCas9*.

Discussion

HyCas9-12aGEP in *C. glutamicum* was developed and optimized to improve the resolution of genome editing. Leveraging hfgRNA design, HyCas9-12aGEP outperforms both CRISPR-Cas9 and CRISPR-Cas12a in terms of gene editing efficiency and active gRNA mapping. HyCas9-12aGEP's robust capability for large-fragment editing enables rapid identification of genotype-phenotype relationships among over 40 genes. Integrating *SpCas9* expression into the genome effectively minimizes off-target editing. In summary, HyCas9-12aGEP streamlines gene editing in *C. glutamicum*, enhancing accessibility and promoting a more sustainable, efficient, and precise biological production process.

SpRY-HF1, an unconstrained near-PAMless and high-fidelity *SpCas9* variant, was inferred to have low nuclease activity in *C. glutamicum* as it is the active gRNA for *SpCas9* but not for SpRY-HF1 and its expression level in *C. glutamicum* is also comparable to *SpCas9*. *SpCas9*/gRNA exhibits stable DNA binding with just an 8-9 bp match to the PAM-proximal region (Singh et al., 2018). However, the SpRY-Cas9 variant, which is generally unrestricted by PAM sites, indicates that a large number of SpRY-Cas9/sgRNA complexes will be titrated on the numerous homologous sequences in the genome. In effect, there were significant reductions in effective SpRY-Cas9/gRNA complex concentrations, which prolong the time for it to search for the target site. Consequently, this decreases the editing activity of the gRNA (Moreb and Lynch, 2021). Meanwhile, the conformational state of the HNH nuclease domain directly controls the DNA cleavage activity, in which the DNA cleavage efficiency is proportional to the extent of the activated conformation of the HNH domain (Sternberg et al., 2015). For *SpCas9*, the HNH-activated conformation is closely linked to the unwinding state of the DNA target, accounting for 78%–100% of the unwinding portion of all DNA targets (Dagdas et al., 2017). *SpCas9*-HF1 also has a reduced ability to unwind target DNA (Okafor et al., 2019), which inevitably inhibits DNA cleavage activity. The titration effect of SpRY-Cas9 and the reduced cleavage efficiency of high-fidelity *SpCas9*-HF1 may have potentially resulted in significant reductions of SpRY-HF1 nuclease activity in *C. glutamicum*.

We attempted unsuccessfully to transform plasmids pFSC-Cas12a and pYJS3-Cas9, which co-express *SpCas9* and *FnCas12a*, into *C. glutamicum*. Plasmids expressing dCas9 in constitutive forms have been challenging to transform in *C. glutamicum* (Cleto et al., 2016). However, optimizing promoters and ribosomal binding sites (RBS) has significantly improved transformation efficiency by reducing *SpCas9* and *FnCas12a* expression (Cleto et al., 2016; Liu et al., 2017; Li et al., 2020). Furthermore, integrating one copy of the *SpCas9* gene into the genome has effectively mitigated the toxicity of *SpCas9* proteins with minimal impact on bacterial growth (Wang et al., 2018). The plasmid copy number is governed by the replicon, with pJYS3 and pFSC plasmids' replicon, *pBL1*, having a range of 10–30 copies (Pátek and Nešvera, 2013). This elevated *SpCas9* or *FnCas12a* expression resulting from the multi-copy *cas* gene could

potentially lead to cytotoxicity. Therefore, this explains why a single copy integration of the *SpCas9* or *FnCas12a* gene does not result in cytotoxicity, while having two copies of either *SpCas9* or *FnCas12a* genes does. Although high concentrations of *SpCas9* proteins can induce cytotoxicity (Cleto et al., 2016) and off-target effects (Hsu et al., 2013; Pattanayak et al., 2013), low-level *SpCas9* or *FnCas12a* expression reduces editing efficiency (Wang et al., 2018) (Figures 1E,F). Therefore, optimizing the expression levels of *SpCas9* or *FnCas12a* proteins is a crucial step in enhancing gene editing efficiency.

The target sites (PAM sites of 5'-NGG-3' and 5'-TTN-3') that HyCas9-12aGEP can use are the sum of *SpCas9* and *FnCas12a*, thereby improving gene editing resolution compared to CRISPR-Cas9 or Cas12a. Although this study demonstrates that the *SpCas9* system can accurately introduce mutations at amino acid 149 of ProB, *FnCas12a* cannot. However, we also found that the gRNA activity of *SpCas9* is diverse in our experiments (Figure 2C, Figures 3C–E), consistent with previous reports (Doench et al., 2014; Moreb and Lynch, 2021; Corsi et al., 2022). In addition, Cas12a has been reported to be more efficient at cutting covalently modified DNA duplexes than Cas9 (Vlot et al., 2018; Dong et al., 2021). Covalent DNA modifications are prevalent across organisms, giving Cas12a an edge over Cas9 when targeting sites within covalently modified genomes. Based on these analyses, the HyCas9-12aGEP improved the resolution of gene editing compared to the CRISPR-Cas9 and Cas12a gene-editing systems. With the discovery of novel Cas proteins (Pausch et al., 2020; Karvelis et al., 2021; Ozcan et al., 2021; Wu et al., 2021; Tsuchida et al., 2022) and application of modified high-performance variants (Kleinstiver et al., 2019; DeWeirdt et al., 2021) in *C. glutamicum*, integration into the genome can further improve gene editing resolution and editing efficiency to build higher-dimensional CRISPR systems.

Based on hfgRNA, HyCas9-12aGEP significantly improves gene editing efficiency compared to classical CRISPR-Cas9 and CRISPR-Cas12a gene editing tools. Previously described CRISPR-Cas9 or Cas12a-based multi-targeting strategies co-expressed pairs of Cas9 (Liu et al., 2017; Horlbeck et al., 2018; Zhao et al., 2018; Zhao et al., 2020) or Cas12a gRNA (Campa et al., 2019; Liu et al., 2019), however, these approaches have limited efficiency, especially in synchronous targeting. Meanwhile, some systems employing orthologous *Staphylococcus aureus* Cas9 and *SpCas9* enzymes (Najm et al., 2017; Boettcher et al., 2018) or *SpCas9* and *Lachnospiraceae bacterium* Cas12a (Gonatopoulos-Pournatzis et al., 2020), like HyCas9-12aGEP, have increased editing efficiency, possibly due to reduced recombination through the use of different transactivating CRISPR RNAs. Taken together, HyCas9-12aGEP greatly improve our capability in terms of genome reprogramming in *C. glutamicum*. Furthermore, we envision that HyCas9-12aGEP is also applicable to other microorganisms.

An efficient gene editing system should not only have reliable and efficient on-target gene editing efficiency, but also should produce minimal off-target effects. It is reported that high levels of Cas9 protein expression would increase the off-target effects (Hsu et al., 2013). In this study, the expression of *SpCas9*/*FnCas12a* protein was reduced by integrating *SpCas9*/*FnCas12a* gene into genome, which was beneficial to reduce the probability of off-target. Indeed, our resequencing results confirmed that

HyCas9-12aGEP did not induce off-target editing at the previously identified *porB* off-target sites (Peng et al., 2017). Although the use of hfgRNA in HyCas9-12aGEP for gene editing theoretically raises the probability of off-target effects, our resequencing results for 9-12Δ*porB*, 9-12Δ*cg0697-0740* and 9-12Δ*gdh::rocG* strains did not reveal any off-target editing. In the further research, it will theoretically contribute to reducing the potential for off-target effects by replacing the high-fidelity Cas9 and Cas12a variants (Chen et al., 2017).

Data availability statement

The datasets presented in this study can be found in online repositories. The names of the repository/repositories and accession number(s) can be found in the article/Supplementary Material.

Author contributions

FZ: Writing–review and editing, Writing–original draft, Validation, Software, Methodology, Investigation, Formal Analysis, Data curation. J-YW: Software, Data curation, Writing–review and editing, Formal Analysis. C-LL: Writing–review and editing, Formal Analysis. W-GZ: Writing–review and editing, Funding acquisition, Formal Analysis.

Funding

The author(s) declare financial support was received for the research, authorship, and/or publication of this article. This work

References

- Abdel-Mawgoud, A. M., and Stephanopoulos, G. (2020). Improving CRISPR/Cas9-mediated genome editing efficiency in *Yarrowia lipolytica* using direct tRNA-sgRNA fusions. *Metab. Eng.* 62, 106–115. doi:10.1016/j.ymben.2020.07.008
- Akhtar, W., de Jong, J., Pindyurin, A., Pagie, L., Meuleman, W., de Ridder, J., et al. (2013). Chromatin position effects assayed by thousands of reporters integrated in parallel. *Cell* 154, 914–927. doi:10.1016/j.cell.2013.07.018
- Becker, J., Rohles, C. M., and Wittmann, C. (2018). Metabolically engineered *Corynebacterium glutamicum* for bio-based production of chemicals, fuels, materials, and healthcare products. *Metab. Eng.* 50, 122–141. doi:10.1016/j.ymben.2018.07.008
- Boettcher, M., Tian, R., Blau, J. A., Markegard, E., Wagner, R. T., Wu, D., et al. (2018). Dual gene activation and knockout screen reveals directional dependencies in genetic networks. *Nat. Biotechnol.* 36, 170–178. doi:10.1038/nbt.4062
- Bryant, J. A., Sellars, L. E., Busby, S. J., and Lee, D. J. (2014). Chromosome position effects on gene expression in *Escherichia coli* K-12. *Nucleic Acids Res.* 42, 11383–11392. doi:10.1093/nar/gku828
- Campa, C. C., Weisbach, N. R., Santinha, A. J., Incarnato, D., and Platt, R. J. (2019). Multiplexed genome engineering by Cas12a and CRISPR arrays encoded on single transcripts. *Nat. Methods* 16, 887–893. doi:10.1038/s41592-019-0508-6
- Chen, J. S., Dagdas, Y. S., Kleinstiver, B. P., Welch, M. M., Sousa, A. A., Harrington, L. B., et al. (2017). Enhanced proofreading governs CRISPR-Cas9 targeting accuracy. *Nature* 550, 407–410. doi:10.1038/nature24268
- Chen, X., Rinsma, M., Janssen, J. M., Liu, J., Maggio, I., and Gonçalves, M. A. (2016). Probing the impact of chromatin conformation on genome editing tools. *Nucleic Acids Res.* 44, 6482–6492. doi:10.1093/nar/gkw524
- Cleto, S., Jensen, J. V. K., Wendisch, V. F., and Lu, T. K. (2016). *Corynebacterium glutamicum* metabolic engineering with CRISPR interference (CRISPRi). *ACS Synth. Biol.* 5, 375–385. doi:10.1021/acssynbio.5b00216
- Cong, L., Ran, F. A., Cox, D., Lin, S., Barretto, R., Habib, N., et al. (2013). Multiplex genome engineering using CRISPR/cas systems. *Science* 339, 819–823. doi:10.1126/science.1231143
- Corsi, G. I., Qu, K., Alkan, F., Pan, X., Luo, Y., and Gorodkin, J. (2022). CRISPR/Cas9 gRNA activity depends on free energy changes and on the target PAM context. *Nat. Commun.* 13, 3006. doi:10.1038/s41467-022-30515-0
- Creutzburg, S. C. A., Wu, W. Y., Mohanraju, P., Swartjes, T., Alkan, F., Gorodkin, J., et al. (2020). Good guide, bad guide: spacer sequence-dependent cleavage efficiency of Cas12a. *Nucleic Acids Res.* 48, 3228–3243. doi:10.1093/nar/gkz1240
- Dagdas Ys, C. J., Sternberg, S. H., Doudna, J. A., and Yildiz, A. (2017). A conformational checkpoint between DNA binding and cleavage by CRISPR-Cas9. *Sci. Adv.* 3, eaa0027. doi:10.1126/sciadv.aao0027
- DeWeirdt, P. C., Sanson, K. R., Sangree, A. K., Hegde, M., Hanna, R. E., Feeley, M. N., et al. (2021). Optimization of AsCas12a for combinatorial genetic screens in human cells. *Nat. Biotechnol.* 39, 94–104. doi:10.1038/s41587-020-0600-6
- Doench, J. G., Hartenian, E., Graham, D. B., Tothova, Z., Hegde, M., Smith, I., et al. (2014). Rational design of highly active sgRNAs for CRISPR-Cas9-mediated gene inactivation. *Nat. Biotechnol.* 32, 1262–1267. doi:10.1038/nbt.3026
- Dong, J., Chen, C., Liu, Y., Zhu, J., Li, M., Rao, V. B., et al. (2021). Engineering T4 bacteriophage for *in vivo* display by type V CRISPR-cas genome editing. *ACS Synth. Biol.* 10, 2639–2648. doi:10.1021/acssynbio.1c00251
- Gonatosopoulos-Pournatzis, T., Aregger, M., Brown, K. R., Farhangmehr, S., Braunschweig, U., Ward, H. N., et al. (2020). Genetic interaction mapping and exon-resolution functional genomics with a hybrid Cas9–Cas12a platform. *Nat. Biotechnol.* 38, 638–648. doi:10.1038/s41587-020-0437-z
- Gong, S., Yu, H. H., Johnson, K. A., and Taylor, D. W. (2018). DNA unwinding is the primary determinant of CRISPR-cas9 activity. *Cell Rep.* 22, 359–371. doi:10.1016/j.celrep.2017.12.041

was supported by the National Key Research and Development Program of China (No. 2021YFC2100900).

Acknowledgments

We thank to Prof. Z. H. Bai from National Engineering Laboratory for Cereal Fermentation Technology, Jiangnan University for donating the plasmids pFSC and pFST-*porB*.

Conflict of interest

The authors declare that the research was conducted in the absence of any commercial or financial relationships that could be construed as a potential conflict of interest.

Publisher's note

All claims expressed in this article are solely those of the authors and do not necessarily represent those of their affiliated organizations, or those of the publisher, the editors and the reviewers. Any product that may be evaluated in this article, or claim that may be made by its manufacturer, is not guaranteed or endorsed by the publisher.

Supplementary material

The Supplementary Material for this article can be found online at: <https://www.frontiersin.org/articles/10.3389/fbioe.2024.1327172/full#supplementary-material>

- Goomans, A. R., Snoeck, N., Decadt, H., Vermeulen, K., Peters, G., Coussemant, P., et al. (2020). Comprehensive study on *Escherichia coli* genomic expression: does position really matter? *Metab. Eng.* 62, 10–19. doi:10.1016/j.ymben.2020.07.007
- Guo, C., Ma, X., Gao, F., and Guo, Y. (2023). Off-target effects in CRISPR/Cas9 gene editing. *Front. Bioeng. Biotechnol.* 11, 1143157. doi:10.3389/fbioe.2023.1143157
- Guo, J., Wang, T., Guan, C., Liu, B., Luo, C., Xie, Z., et al. (2018). Improved sgRNA design in bacteria via genome-wide activity profiling. *Nucleic Acids Res.* 46, 7052–7069. doi:10.1093/nar/gky572
- Horlbeck, M. A., Witkowski, L. B., Guglielmi, B., Replogle, J. M., Gilbert, L. A., Villalta, J. E., et al. (2016). Nucleosomes impede Cas9 access to DNA *in vivo* and *in vitro*. *Elife* 5, e12677. doi:10.7554/elifelife.12677
- Horlbeck, M. A., Xu, A., Wang, M., Bennett, N. K., Park, C. Y., Bogdanoff, D., et al. (2018). Mapping the genetic landscape of human cells. *Cell* 174, 953–967. doi:10.1016/j.cell.2018.06.010
- Hsu, P. D., Scott, D. A., Weinstein, J. A., Ran, F. A., Konermann, S., Agarwala, V., et al. (2013). DNA targeting specificity of RNA-guided Cas9 nucleases. *Nat. Biotechnol.* 31, 827–832. doi:10.1038/nbt.2647
- Ivanov, I. E., Wright, A. V., Cofsky, J. C., Aris, K. D. P., Doudna, J. A., and Bryant, Z. (2020). Cas9 interrogates DNA in discrete steps modulated by mismatches and supercoiling. *Proc. Natl. Acad. Sci. U. S. A.* 117, 5853–5860. doi:10.1073/pnas.1913445117
- Jiang, W., Bikard, D., Cox, D., Zhang, F., and Marraffini, L. A. (2013). RNA-guided editing of bacterial genomes using CRISPR-Cas systems. *Nat. Biotechnol.* 31, 233–239. doi:10.1038/nbt.2508
- Jiang, Y., Qian, F., Yang, J., Liu, Y., Dong, F., Xu, C., et al. (2017). CRISPR-Cpf1 assisted genome editing of *Corynebacterium glutamicum*. *Nat. Commun.* 8, 15179–15189. doi:10.1038/ncomms15179
- Jinek, M., Chylinski, K., Fonfara, I., Hauer, M., Doudna, J. A., and Charpentier, E. (2012). A programmable dual-RNA-guided DNA endonuclease in adaptive bacterial immunity. *Science* 337, 816–821. doi:10.1126/science.1225829
- Karvelis, T., Druiteika, G., Bigelyte, G., Budre, K., Zedaveinyte, R., Silanskas, A., et al. (2021). Transposon-associated TnpB is a programmable RNA-guided DNA endonuclease. *Nature* 599, 692–696. doi:10.1038/s41586-021-04058-1
- Kim, H. K., Min, S., Song, M., Jung, S., Choi, J. W., Kim, Y., et al. (2018). Deep learning improves prediction of CRISPR-Cpf1 guide RNA activity. *Nat. Biotechnol.* 36, 239–241. doi:10.1038/nbt.4061
- Kim, N., Kim, H. K., Lee, S., Seo, J. H., Choi, J. W., Park, J., et al. (2020). Prediction of the sequence-specific cleavage activity of Cas9 variants. *Nat. Biotechnol.* 38, 1328–1336. doi:10.1038/s41587-020-0537-9
- Kleine, B., Chattopadhyay, A., Polen, T., Pinto, D., Mascher, T., Bott, M., et al. (2017). The three-component system EsrISR regulates a cell envelope stress response in *Corynebacterium glutamicum*. *Mol. Microbiol.* 106, 719–741. doi:10.1111/mmi.13839
- Kleinstiver, B. P., Sousa, A. A., Walton, R. T., Tak, Y. E., Hsu, J. Y., Clement, K., et al. (2019). Engineered CRISPR-Cas12a variants with increased activities and improved targeting ranges for gene, epigenetic and base editing. *Nat. Biotechnol.* 37, 276–282. doi:10.1038/s41587-018-0011-0
- Kudla, G., Murray, A. W., Tollervey, D., and Plotkin, J. B. (2009). Coding-sequence determinants of gene expression in *Escherichia coli*. *Science* 324, 255–258. doi:10.1126/science.1170160
- Li, M., Chen, J., Wang, Y., Liu, J., Huang, J., Chen, N., et al. (2020). Efficient multiplex gene repression by CRISPR-dCpf1 in *Corynebacterium glutamicum*. *Front. Bioeng. Biotechnol.* 8, 357. doi:10.3389/fbioe.2020.00357
- Liu, J., Liu, M., Shi, T., Sun, G., Gao, N., Zhao, X., et al. (2022). CRISPR-assisted rational flux-tuning and arrayed CRISPRi screening of an L-proline exporter for L-proline hyperproduction. *Nat. Commun.* 13, 891–906. doi:10.1038/s41467-022-28501-7
- Liu, J., Srinivasan, S., Li, C. Y., Ho, I. L., Rose, J., Shaheen, M., et al. (2019). Pooled library screening with multiplexed Cpf1 library. *Nat. Commun.* 10, 3144. doi:10.1038/s41467-019-10963-x
- Liu, J., Wang, Y., Lu, Y., Zheng, P., Sun, J., and Ma, Y. (2017). Development of a CRISPR/Cas9 genome editing toolbox for *Corynebacterium glutamicum*. *Microb. Cell Fact.* 16, 205. doi:10.1186/s12934-017-0815-5
- Liu, Y. D. L., Dong, J., Chen, C., Zhu, J., Rao, V. B., Tao, P., et al. (2020). Covalent modifications of the bacteriophage genome confer a degree of resistance to bacterial CRISPR systems. *J. Virol.* 94, e01630. doi:10.1128/jvi.01630-20
- Magnusson, J. P., Rios, A. R., Wu, L., and Qi, L. S. (2021). Enhanced Cas12a multi-gene regulation using a CRISPR array separator. *Elife* 10, e66406. doi:10.7554/elifelife.66406
- Moreb, E. A., Huttmacher, M., and Lynch, M. D. (2020). CRISPR-cas "Non-Target" sites inhibit on-target cutting rates. *CRISPR J.* 3, 550–561. doi:10.1089/crispr.2020.0065
- Moreb, E. A., and Lynch, M. D. (2021). Genome dependent Cas9/gRNA search time underlies sequence dependent gRNA activity. *Nat. Commun.* 12, 5034. doi:10.1038/s41467-021-25339-3
- Najm, F. J., Strand, C., Donovan, K. F., Hegde, M., Sanson, K. R., Vaimberg, E. W., et al. (2017). Orthologous CRISPR-Cas9 enzymes for combinatorial genetic screens. *Nat. Biotechnol.* 36, 179–189. doi:10.1038/nbt.4048
- Okafor, I. C., Singh, D., Wang, Y., Jung, M., Wang, H., Mallon, J., et al. (2019). Single molecule analysis of effects of non-canonical guide RNAs and specificity-enhancing mutations on Cas9-induced DNA unwinding. *Nucleic Acids Res.* 47, 11880–11888. doi:10.1093/nar/gkz1058
- Ozcan, A., Krajeski, R., Ioannidi, E., Lee, B., Gardner, A., Makarova, K. S., et al. (2021). Programmable RNA targeting with the single-protein CRISPR effector Cas7-11. *Nature* 597, 720–725. doi:10.1038/s41586-021-03886-5
- Pan, X., Tang, M., You, J., Osire, T., Sun, C., Fu, W., et al. (2022). PsrA is a novel regulator contributes to antibiotic synthesis, bacterial virulence, cell motility and extracellular polysaccharides production in *Serratia marcescens*. *Nucleic Acids Res.* 50, 127–148. doi:10.1093/nar/gkab1186
- Park, J., Lim, J. M., Jung, I., Heo, S. J., Park, J., Chang, Y., et al. (2021). Recording of elapsed time and temporal information about biological events using Cas9. *Cell* 184, 1047–1063. doi:10.1016/j.cell.2021.01.014
- Park, J. B. S., and Kim, J. S. (2015). Cas-Designer: a web-based tool for choice of CRISPR-Cas9 target sites. *Bioinformatics* 31, 4014–4016. doi:10.1093/bioinformatics/btv537
- Pátek, M., and Nešvera, J. (2013). *Corynebacterium glutamicum* Biology and Biotechnology. Berlin, Germany: Springer, 51–88.
- Pattanayak, V., Lin, S., Guillinger, J. P., Ma, E., Doudna, J. A., and Liu, D. R. (2013). High-throughput profiling of off-target DNA cleavage reveals RNA-programmed Cas9 nuclease specificity. *Nat. Biotechnol.* 31, 839–843. doi:10.1038/nbt.2673
- Pausch, P., Al-Shayeb, B., Bisom-Rapp, E., Tsuchida, C. A., Li, Z., Cress, B. F., et al. (2020). CRISPR-CasΦ from huge phages is a hypercompact genome editor. *Science* 369, 333–337. doi:10.1126/science.abb1400
- Peng, F., Wang, X., Sun, Y., Dong, G., Yang, Y., Liu, X., et al. (2017). Efficient gene editing in *Corynebacterium glutamicum* using the CRISPR/Cas9 system. *Microb. Cell Fact.* 16, 201. doi:10.1186/s12934-017-0814-6
- Perez-Arellano, I., Rubio, V., and Cervera, J. (2006). Mapping active site residues in glutamate-5-kinase. The substrate glutamate and the feed-back inhibitor proline bind at overlapping sites. *FEBS Lett.* 580, 6247–6253. doi:10.1016/j.febslet.2006.10.031
- Resende, B. C., Rebelato, A., D'Afonseca, V., Santos, A., Stutzman, T., Azevedo, V., et al. (2011). DNA repair in *Corynebacterium* model. *Gene* 482, 1–7. doi:10.1016/j.gene.2011.03.008
- Riesenberg, S., Helmbrecht, N., Kanis, P., Maricic, T., and Paabo, S. (2022). Improved gRNA secondary structures allow editing of target sites resistant to CRISPR-Cas9 cleavage. *Nat. Commun.* 13, 489. doi:10.1038/s41467-022-28137-7
- Singh, D., Wang, Y., Mallon, J., Yang, O., Fei, J., Poddar, A., et al. (2018). Mechanisms of improved specificity of engineered Cas9s revealed by single-molecule FRET analysis. *Nat. Struct. Mol. Biol.* 25, 347–354. doi:10.1038/s41594-018-0051-7
- Sternberg, S. H., LaFrance, B., Kaplan, M., and Doudna, J. A. (2015). Conformational control of DNA target cleavage by CRISPR-Cas9. *Nature* 527, 110–113. doi:10.1038/nature15544
- Sternberg, S. H., Redding, S., Jinek, M., Greene, E. C., and Doudna, J. A. (2014). DNA interrogation by the CRISPR RNA-guided endonuclease Cas9. *Nature* 507, 62–67. doi:10.1038/nature13011
- Talas, A., Huszár, K., Kulcsár, P. I., Varga, J. K., Varga, É., Tóth, E., et al. (2021). A method for characterizing Cas9 variants via a one-million target sequence library of self-targeting sgRNAs. *Nucleic Acids Res.* 49, e31. doi:10.1093/nar/gkaa1220
- Tao, P., Wu, X., Tang, W. C., Zhu, J., and Rao, V. (2017). Engineering of bacteriophage T4 genome using CRISPR-cas9. *ACS Synth. Biol.* 6, 1952–1961. doi:10.1021/acssynbio.7b00179
- Tsuchida, C. A., Zhang, S., Doost, M. S., Zhao, Y., Wang, J., O'Brien, E., et al. (2022). Chimeric CRISPR-CasX enzymes and guide RNAs for improved genome editing activity. *Mol. Cell* 82, 1199–1209. doi:10.1016/j.molcel.2022.02.002
- Vlot, M., Houkes, J., Lochs, S. J., Swarts, D. C., Zheng, P., Kunne, T., et al. (2018). Bacteriophage DNA glucosylation impairs target DNA binding by type I and II but not by type V CRISPR-Cas effector complexes. *Nucleic Acids Res.* 46, 873–885. doi:10.1093/nar/gkx1264
- Walton Rt, C. K., Whittaker, M. N., and Kleinstiver, B. P. (2020). Unconstrained genome targeting with near-PAMless engineered CRISPR-Cas9 variants. *Science* 368, 290–296. doi:10.1126/science.aba8853
- Wang, B., Hu, Q., Zhang, Y., Shi, R., Chai, X., Liu, Z., et al. (2018). A RecET-assisted CRISPR-Cas9 genome editing in *Corynebacterium glutamicum*. *Microb. Cell Fact.* 17, 63. doi:10.1186/s12934-018-0910-2
- Wang, D., Zhang, C., Wang, B., Li, B., Wang, Q., Liu, D., et al. (2019). Optimized CRISPR guide RNA design for two high-fidelity Cas9 variants by deep learning. *Nat. Commun.* 10, 4284. doi:10.1038/s41467-019-12281-8
- Wang, M., Chen, B., Fang, Y., and Tan, T. (2017). Cofactor engineering for more efficient production of chemicals and biofuels. *Biotechnol. Adv.* 35, 1032–1039. doi:10.1016/j.biotechadv.2017.09.008

- Wang, Y., Cheng, H., Liu, Y., Liu, Y., Wen, X., Zhang, K., et al. (2021). *In-situ* generation of large numbers of genetic combinations for metabolic reprogramming via CRISPR-guided base editing. *Nat. Commun.* 12, 678. doi:10.1038/s41467-021-21003-y
- Wang, Y. Y., Shi, K., Chen, P., Zhang, F., Xu, J. Z., and Zhang, W. G. (2020). Rational modification of the carbon metabolism of *Corynebacterium glutamicum* to enhance L-leucine production. *J. Ind. Microbiol. Biotechnol.* 47, 485–495. doi:10.1007/s10295-020-02282-8
- Wendisch, V. F. (2014). Microbial production of amino acids and derived chemicals: synthetic biology approaches to strain development. *Curr. Opin. Biotechnol.* 30, 51–58. doi:10.1016/j.copbio.2014.05.004
- Wienert, B., and Cromer, M. K. (2022). CRISPR nuclease off-target activity and mitigation strategies. *Front. Genome Ed.* 4, 1050507. doi:10.3389/fgeed.2022.1050507
- Wolf, S., Becker, J., Tsuge, Y., Kawaguchi, H., Kondo, A., Marienhagen, J., et al. (2021). Advances in metabolic engineering of *Corynebacterium glutamicum* to produce high-value active ingredients for food, feed, human health, and well-being. *Essays Biochem.* 65, 197–212. doi:10.1042/ebc20200134
- Wu, Z., Zhang, Y., Yu, H., Pan, D., Wang, Y., Wang, Y., et al. (2021). Programmed genome editing by a miniature CRISPR-Cas12f nuclease. *Nat. Chem. Biol.* 17, 1132–1138. doi:10.1038/s41589-021-00868-6
- Xiang, X., Corsi, G. I., Anthon, C., Qu, K., Pan, X., Liang, X., et al. (2021). Enhancing CRISPR-Cas9 gRNA efficiency prediction by data integration and deep learning. *Nat. Commun.* 12, 3238. doi:10.1038/s41467-021-23576-0
- Xu, J. X., Zhang, J., Guo, Y., Qian, H., and Zhang, W. (2014). A method for gene amplification and simultaneous deletion in *Corynebacterium glutamicum* genome without any genetic markers. *Plasmid* 72, 9–17. doi:10.1016/j.plasmid.2014.02.001
- Yan, M. Y., Yan, H. Q., Ren, G. X., Zhao, J. P., Guo, X. P., and Sun, Y. C. (2017). CRISPR-Cas12a-Assisted recombineering in bacteria. *Appl. Environ. Microbiol.* 83, e00947–e00917. doi:10.1128/aem.00947-17
- Yarrington, R. M., Verma, S., Schwartz, S., Trautman, J. K., and Carroll, D. (2018). Nucleosomes inhibit target cleavage by CRISPR-Cas9 *in vivo*. *Proc. Natl. Acad. Sci. U. S. A.* 115, 9351–9358. doi:10.1073/pnas.1810062115
- Yim, S. S., An, S. J., Kang, M., Lee, J., and Jeong, K. J. (2013). Isolation of fully synthetic promoters for high-level gene expression in *Corynebacterium glutamicum*. *Biotechnol. Bioeng.* 110, 2959–2969. doi:10.1002/bit.24954
- Zetsche, B., Gootenberg, J., Abudayyeh, O., Slaymaker, I., Makarova, K., Essletzbichler, P., et al. (2015). Cpf1 is a single RNA-guided endonuclease of a class 2 CRISPR-cas system. *Cell* 163, 759–771. doi:10.1016/j.cell.2015.09.038
- Zetsche, B., Heidenreich, M., Mohanraju, P., Fedorova, I., Kneppers, J., DeGennaro, E. M., et al. (2017). Multiplex gene editing by CRISPR-Cpf1 using a single crRNA array. *Nat. Biotechnol.* 35, 31–34. doi:10.1038/nbt.3737
- Zhang, J., Qian, F., Dong, F., Wang, Q., Yang, J., Jiang, Y., et al. (2020). *De novo* engineering of *Corynebacterium glutamicum* for l-proline production. *ACS Synth. Biol.* 9, 1897–1906. doi:10.1021/acssynbio.0c00249
- Zhao, D., Badur, M. G., Luebeck, J., Magaña, J. H., Birmingham, A., Sasik, R., et al. (2018). Combinatorial CRISPR-cas9 metabolic screens reveal critical redox control points dependent on the KEAP1-NRF2 regulatory Axis. *Mol. Cell* 69, 699–708. doi:10.1016/j.molcel.2018.01.017
- Zhao, N., Li, L., Luo, G., Xie, S., Lin, Y., Han, S., et al. (2020). Multiplex gene editing and large DNA fragment deletion by the CRISPR/Cpf1-RecE/T system in *Corynebacterium glutamicum*. *J. Ind. Microbiol. Biotechnol.* 47, 599–608. doi:10.1007/s10295-020-02304-5